Passive harmonic hybrid mode-locked fiber laser with extremely broad spectrum

Xing Li,[1,2,3] Weiwen Zou,[1,2,*] and Jianping Chen[1,2]

[1]*State Key Laboratory of Advanced Optical Communication Systems and Networks, Department of Electronic Engineering, Shanghai Jiao Tong University, Shanghai 200240, China*
[2]*Shanghai Key Lab of Navigation and Location Services, Shanghai Jiao Tong University, Shanghai 200240, China*
[3]*Laboratory of Infrared Materials and Devices, The Research Institute of Advanced Technologies, Ningbo University, Ningbo 315211, China*
*wzou@sjtu.edu.cn

Abstract: We demonstrate a harmonic mode-locking Erbium-doped fiber laser which is cooperatively mode-locked by nonlinear polarization evolution (NPE) and semiconductor saturable absorber mirror (SESAM). Via effective dispersion and nonlinearity optimization, 8th harmonic at a repetition rate of 666.7 MHz is obtained. The output pulses has a full spectrum width at half maximum (FWHM) of 181 nm and duration of 218 *fs*. The pulses are compressed to 91 *fs* by external chirp compensation. The average power of the direct output pulse at an available pump power of 1.5 W is 136 mW, which exhibits a single-pulse energy of 0.2 nJ. The cavity super-mode suppression is up to 60 dB and the signal-to-noise ratio of the 8th harmonic is over 75 dB.

OCIS codes: (140.3510) Lasers, fiber; (140.4050) Mode-locked lasers; (140.7090) Ultrafast lasers.

References and links

1. G. C. Valley, "Photonic analog-to-digital converters," Opt. Express **15**(5), 1955–1982 (2007).
2. G. Wu, S. Li, X. Li, and J. Chen, "18 wavelengths 83.9Gs/s optical sampling clock for photonic A/D converters," Opt. Express **18**(20), 21162–21168 (2010).
3. J. Rauschenberger, T. Fortier, D. Jones, J. Ye, and S. Cundiff, "Control of the frequency comb from a modelocked Erbium-doped fiber laser," Opt. Express **10**(24), 1404–1410 (2002).
4. S. T. Cundiff and A. M. Weiner, "Optical arbitrary waveform generation," Nat. Photonics **4**(11), 760–766 (2010).
5. B. E. Bouma, L. E. Nelson, G. J. Tearney, D. J. Jones, M. E. Brezinski, and J. G. Fujimoto, "Optical Coherence Tomographic Imaging of Human Tissue at 1.55 μm and 1.81 μm Using Er- and Tm-Doped Fiber Sources," J. Biomed. Opt. **3**(1), 76–79 (1998).
6. J. Xu, C. Zhang, J. Xu, K. K. Y. Wong, and K. K. Tsia, "Megahertz all-optical swept-source optical coherence tomography based on broadband amplified optical time-stretch," Opt. Lett. **39**(3), 622–625 (2014).
7. A. B. Grudinin and S. Gray, "Passive harmonic mode locking in soliton fiber lasers," J. Opt. Soc. Am. B **14**(1), 144–154 (1997).
8. J. N. Kutz, B. Collings, K. Bergman, and W. Knox, "Stabilized pulse spacing in soliton lasers due to gain depletion and recovery," IEEE J. Quantum Electron. **34**(9), 1749–1757 (1998).
9. J. P. Gordon, "Dispersive perturbations of solitons of the nonlinear Schrödinger equation," J. Opt. Soc. Am. B **9**(1), 91–97 (1992).
10. A. B. Grudinin, D. J. Richardson, and D. N. Payne, "Passive harmonic mode locking of a fibre soliton ring laser," Electron. Lett. **29**(21), 1860–1861 (1993).
11. Z. X. Zhang, Z. Q. Ye, M. H. Sang, and Y. Y. Nie, "Passively mode-locked fiber laser based on symmetrical nonlinear optical loop mirror," Laser Phys. Lett. **5**(5), 364–366 (2008).
12. F. Amrani, A. Haboucha, M. Salhi, H. Leblond, A. Komarov, P. Grelu, and F. Sanchez, "Passively mode-locked erbium-doped double-clad fiber laser operating at the 322nd harmonic," Opt. Lett. **34**(14), 2120–2122 (2009).
13. P. Dmitriy, P. Polynkin, A. Polynkin, J. V. Moloney, M. Mansuripur, and N. Peyghambarian, "Er-Yb femtosecond ring fiber oscillator with 1.1-W average power and GHz repetition rates," IEEE Photon. Technol. Lett. **18**(7), 853–855 (2006).
14. C. Lecaplain and P. Grelu, "Multi-gigahertz repetition-rate-selectable passive harmonic mode locking of a fiber laser," Opt. Express **21**(9), 10897–10902 (2013).

#243942 Received 30 Jun 2015; revised 31 Jul 2015; accepted 4 Aug 2015; published 6 Aug 2015

15. J. Peng, L. Zhan, S. Luo, and Q. Shen, "Passive harmonic mode-locking of dissipative dolitons in a normal-dispersion Er-doped fiber laser," J. Lightwave Technol. **31**(16), 3009–3014 (2013).
16. Z. X. Zhang, L. Wang, and Y. J. Wang, "Sub-100 fs and passive harmonic mode-locking of dispersion-managed dissipative fiber laser with carbon nanotubes," J. Lightwave Technol. **31**(23), 3719–3725 (2013).
17. B. C. Collings, K. Bergman, and W. H. Knox, "Stable multigigahertz pulse-train formation in a short-cavity passively harmonic mode-locked erbium/ytterbium fiber laser," Opt. Lett. **23**(2), 123–125 (1998).
18. Y. Deng, M. Koch, F. Lu, G. Wicks, and W. Knox, "Colliding-pulse passive harmonic mode-locking in a femtosecond Yb-doped fiber laser with a semiconductor saturable absorber," Opt. Express **12**(16), 3872–3877 (2004).
19. C. Mou, R. Arif, A. Rozhin, and S. Turitsyn, "Passively harmonic mode locked erbium doped fiber soliton laser with carbon nanotubes based saturable absorber," Opt. Mater. Express **2**(6), 884–890 (2012).
20. C. S. Jun, S. Y. Choi, F. Rotermund, B. Y. Kim, and D. I. Yeom, "Toward higher-order passive harmonic mode-locking of a soliton fiber laser," Opt. Lett. **37**(11), 1862–1864 (2012).
21. G. Sobon, J. Sotor, and K. M. Abramski, "Passive harmonic mode-locking in Er-doped fiber laser based on graphene saturable absorber with repetition rates scalable to 2.22 GHz," Appl. Phys. Lett. **100**(16), 161109 (2012).
22. J. Sotor, G. Sobon, W. Macherzynski, and K. M. Abramski, "Harmonically mode-locked Er-doped fiber laser based on a Sb2Te3 topological insulator saturable absorber," Laser Phys. Lett. **11**(5), 055102 (2014).
23. K. S. Abedin, J. T. Gopinath, L. A. Jiang, M. E. Grein, H. A. Haus, and E. P. Ippen, "Self-stabilized passive, harmonically mode-locked stretched-pulse erbium fiber ring laser," Opt. Lett. **27**(20), 1758–1760 (2002).
24. S. W. Chu, T. M. Liu, C. K. Sun, C. Y. Lin, and H. J. Tsai, "Real-time second-harmonic-generation microscopy based on a 2-GHz repetition rate Ti:sapphire laser," Opt. Express **11**(8), 933–938 (2003).
25. X. Li, W. Zou, and J. Chen, "41.9 fs hybridly mode-locked Er-doped fiber laser at 212 MHz repetition rate," Opt. Lett. **39**(6), 1553–1556 (2014).
26. D. Y. Tang and L. M. Zhao, "Generation of 47-fs pulses directly from an erbium-doped fiber laser," Opt. Lett. **32**(1), 41–43 (2007).
27. X. Li, W. Zou, G. Yang, and J. P. Chen, "Direct generation of 148 nm and 44.6 fs pulses in an Erbium-doped fiber laser," IEEE Photonics Technol. Lett. **27**(1), 93–96 (2015).
28. J. J. McFerran, L. Nenadovic, W. C. Swann, J. B. Schlager, and N. R. Newbury, "A passively mode-locked fiber laser at 1.54 μm with a fundamental repetition frequency reaching 2 GHz," Opt. Express **15**(20), 13155–13166 (2007).
29. A. Komarov, H. Leblond, and F. Sanchez, "Multistability and hysteresis phenomena in passively mode-locked fiber lasers," Phys. Rev. A **71**(5), 053809 (2005).
30. Z. X. Zhang, L. Zhan, X. X. Yang, S. Y. Luo, and Y. X. Xia, "Passive harmonically mode-locked erbium-doped fiber laser with scalable repetition rate up to 1.2 GHz," Laser Phys. Lett. **4**(8), 592–596 (2007).
31. X. Zhou, D. Yoshitomi, Y. Kobayashi, and K. Torizuka, "Generation of 28-fs pulses from a mode-locked ytterbium fiber oscillator," Opt. Express **16**(10), 7055–7059 (2008).
32. H. Yang, A. Wang, and Z. Zhang, "Efficient femtosecond pulse generation in an all-normal-dispersion Yb:fiber ring laser at 605 MHz repetition rate," Opt. Lett. **37**(5), 954–956 (2012).

1. Introduction

Femtosecond mode-locking fiber lasers with high repetition rate and broad spectrum have important applications in high-speed optical sampling for photonic analog-to-digital convertors [1,2], frequency comb generation for optical frequency metrology [3], optical arbitrary waveform generation [4], and optical coherence tomography [5,6] etc. High repetition rate pulse trains can be produced from harmonic mode-locking (HML) fiber lasers when pump power exceeds certain threshold and thereafter the relatively high intracavity nonlinearity accumulation leads to the single pulse circulating in the cavity splitting into several pulses. Generally, the split pulses are usually randomly located in the cavity. However, under certain conditions they can self-arrange to create a stable and evenly spaced pulse train with repetition rates far beyond the fundamental repetition rate. Various mechanisms including soliton-dispersive wave interactions [7], the effective repulsion force due to gain depletion and recovery [8], and soliton-soliton attraction or repulsion [9], are responsible for this effect.

Since Grudinin *et al.* first reported the experimental observation of passive harmonic mode-locking (PHML) in an erbium-doped fiber laser [10], PHML has become a well-known phenomenon and has been observed in various types of fiber lasers at 1.5μm wavelength. A lot of PHML techniques, such as nonlinear loop mirror (NOLM) [11], nonlinear polarization evolution (NPE) [12–16], saturable absorbers (SAMs) including both conventional semiconductor saturable absorbers [17, 18] and novel saturable absorber such as carbon-

#243942 Received 30 Jun 2015; revised 31 Jul 2015; accepted 4 Aug 2015; published 6 Aug 2015

nanotube [19, 20], graphene [21], and topological insulator [22] have been successfully demonstrated. However, there are still some issues to be solved. First, the pulse duration is usually more than 100 fs and the spectrum width are limited to a few nanometers in most PHML fiber lasers. Although pulse duration of 125 fs and spectrum width of 50 nm were realized in a stretched-pulse erbium fiber laser at a high repetition rate of 220 MHz [23], it cannot meet the demand of some applications. For example, in applications of high-speed optical sampling based on optical wavelength division multiplexing (WDM) technique [1] or biological imaging [24], the high repetition rate fiber laser with a broadband spectrum larger than 100 nm is highly desired. Second, fast saturable absorber, including NPE and NOLM, is a common method to generate a broad spectrum and thus ultrashort pulses due to the large modulation depth and essentially instantaneous response. However, PHML fiber lasers based on NPE or NOLM are relatively unstable due to polarization drift by environmental disturbance. Although PHML fiber lasers based on slow saturable absorber such as SAMs can easily achieve self-starting and thus mode-locking is comparatively stable, inevitable pulse shaping caused by slow saturable absorbers limits the pulse duration to an order of picosecond and the spectral bandwidth to a few nanometers. In recent years, the novel saturable absorber materials such as carbon-nanotube and graphene which have both fast and slow saturable absorption properties were widely used in PHML fiber lasers, but the spectral bandwidth was still constrained to a few nanometers and thereby a broad pulse was often obtained. To alleviate the above problems, simultaneous application of two mode-locking techniques in one hybrid laser cavity has been developed in a fundamental mode-locking fiber laser, which demonstrates the advantages of both fast and slow saturable absorber [25]. In the case of fixed gain and loss in fiber lasers, the pulse shaping is regulated by the mutual interactions between dispersion and nonlinearity in fiber lasers [26]. We recently demonstrated that the NPE-based fundamental mode-locking fiber laser can produce ultrashort pulse and broadband spectrum under effective dispersion and nonlinearity optimization [27]. It is now of particular interest to know whether dispersion and nonlinearity optimization are also effective in PHML fiber lasers.

In this paper, we demonstrate a harmonic hybrid mode-locking scheme of Erbium-doped fiber laser that incorporates the NPE and SESAM. The NPE is intended to shape ultrashort pulses and broaden the spectrum while the SESAM adopted here enables self-starting. Dispersion and nonlinearity engineering are also carried out in this HML fiber laser. These two improvements result in a 181 nm spectrum width and 218 fs pulse duration with repetition rate of 666.7 MHz at the 8th harmonic. The pulses can be compressed to 91 fs by external chirp compensation. The signal-to-noise ratio (SNR) is better than ~75 dB at the 8th HML, and the super-mode suppression reaches ~60 dB. The laser performances at the 4th harmonic are also discussed.

2. Principle and experimental setup

Figure 1 depicts the sigma configuration of the hybrid HML fiber laser with bidirectional pumps. It is organized by a set of fibers and free-space components under appropriate GVD management. The fibers include a highly Er-doped gain fiber (Liekki ER110-4/125), two OFS-980 fiber pigtails of 980/1550 nm wavelength division multiplexers (WDM1 and WDM2), and two leading fibers (SMF28) of the collimator1 and collimator2. The free-space components comprises of polarization beam splitter (PBS), waveplates, isolator, aspheric lens and SESAM (BATOP GmbH) with a 6% modulation depth, a 2 ps recovery time, and a 50 $\mu J/cm^2$ saturation fluence. The PBS acts both as the polarizer for the NPE mode locking and as the laser output coupler. The polarization-dependent isolator is inserted after the PBS to allow unidirectional operation of the cavity. Note that a polarisation-independent isolator may work equally. The aspheric lens is used to focus the beam (focal length = 11 mm) onto the SESAM. The gain fiber is bidirectionally pumped by two 974 nm laser diodes with a maximum pump power of 1.5 W through the WDMs. The NPE in the cavity is optimized by a

#243942 Received 30 Jun 2015; revised 31 Jul 2015; accepted 4 Aug 2015; published 6 Aug 2015

half waveplate and three quarter waveplates. The laser output is characterized by an autocorrelator (Femtochrome, FR-103XL) and an optical spectrum analyzer (Yokogawa AQ6370C). The pulse output is detected by a 10 GHz photodetector (EOT, ET-3500F), which is analyzed by an 8 GHz oscilloscope (Tektronix DSA70804) and a signal source analyzer (R&S FSUP50).

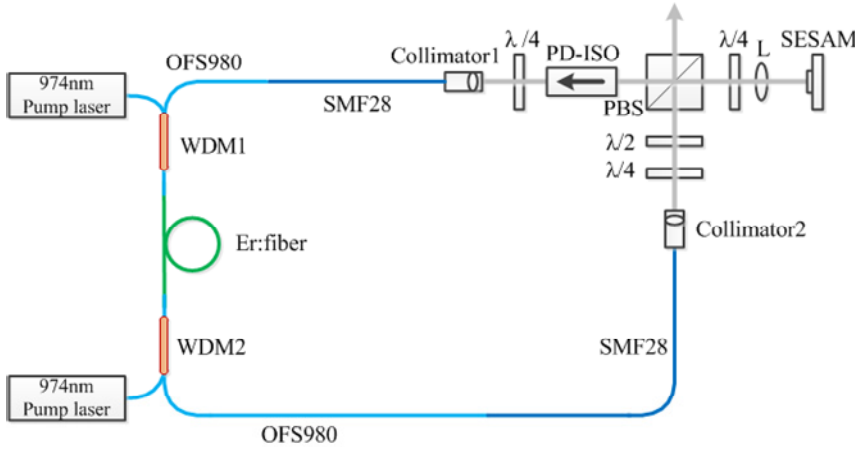

Fig. 1. Configuration of the hybrid HML fiber laser with bidirectional pumps. PBS, polarization beam splitter; PD-ISO, polarization-dependent isolator; λ/2, half waveplate; λ/4, quarter waveplate; L, aspheric lens; WDM, wavelength-division multiplexer.

Table 1. Parameters of all fibers in the hybrid HML cavity with dispersion and nonlinearity optimization.

	Er:fiber	WDM1	WDM2	Collimator1	Collimator2
GVD (fs^2/mm)	11.9	1.8	1.8	–21.7	–21.7
γ (W^{-1}/m)	0.0032	0.0021	0.0021	0.0012	0.0012
Length (mm)	400	480	900	190	300

Usually, setting the total cavity dispersion to zero and reducing the effective cavity nonlinearity are verified as a better way to generate a broadband spectrum and thereby ultrashort pulses [27]. Considering the GVD of SESAM and free-space bulk components, the net GVD of the whole cavity is managed to be close to zero at 1550 nm. Nonlinearity also plays an important role in pulse-forming process. If the accumulated nonlinear phase shift is too small, the HML action of the fiber laser can hardly be implemented in a relatively short cavity under certain pump power. In order to accumulate enough nonlinear phase shifts for HML operated at a high repetition rate, the leading fiber of the collimator1 and the OFS-980 fiber pigtail of the WDM1 should be kept short compared with the OFS-980 fiber pigtail of the WDM2 and the following SMF28 of collimator2. As a result, the accumulation of nonlinear phase shift becomes dominant. The length, GVD coefficients and nonlinearity coefficients of all fibers are summarized in Table 1.

3. Results and discussion

At the threshold total pump power of 320 mW, mode-locking of the laser is easily achieved by adjusting the waveplates. Once set, the single pulse operation is self-starting and highly stable. When the total pump power increases to 400 mW (the backward pump laser is 400 mW and the forward one is 0 mW), the average output power of the mode-locking pulses is 32 mW. Figure 2(a) illustrates equally spaced pulses emitted from the laser with a fundamental repetition rate of 83.3 MHz, suggesting no dual-pulsing or Q-switched mode-

#243942 Received 30 Jun 2015; revised 31 Jul 2015; accepted 4 Aug 2015; published 6 Aug 2015

locking operation of laser oscillator. Figure 2(b) depicts an optical spectrum at the fundamental repetition rate with a spec-

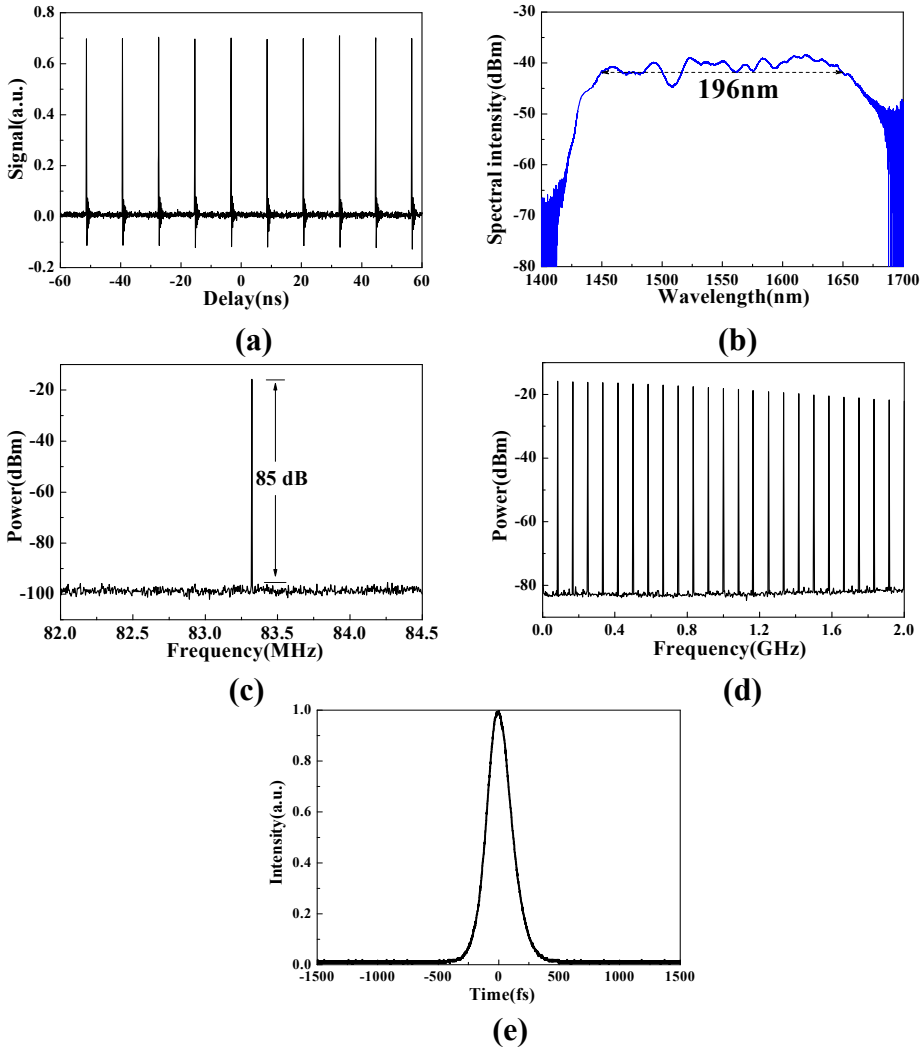

Fig. 2. Fundamental hybrid mode-locking characteristics. (a) Output pulse trains measured by an oscilloscope, (b) optical spectrum measured with 0.02 nm resolution, (c) RF spectrum of fundamental mode beat measured at 300 Hz resolution bandwidth, (d) RF spectrum of harmonics with 2 GHz span measured at 10 kHz resolution bandwidth, and (e) autocorrelation trace of the direct output pulse.

trum resolution of 0.02 nm, which is achieved by adjusting the waveplates under the status that the mode-locking is self-restarted and stable. The spectrum is broad and smooth with a FWHM of about 196 nm (from ~1450 nm to ~1650 nm), which is the typical feature of stretched-pulse lasers and confirms the effectiveness of dispersion management and nonlinearity optimization in the hybrid mode-locking fiber laser. The spectrum is much broader than fiber laser mode-locked just based on SESAM [28]. It indicates that in the hybrid mode-locking mechanism, the main role of the NPE is to shape pulses in pulse-forming process and the SESAM has no evident contribution to pulse shaping. The RF spectrum of the fundamental mode beat is illustrated in Fig. 2(c). The SNR of the

#243942 Received 30 Jun 2015; revised 31 Jul 2015; accepted 4 Aug 2015; published 6 Aug 2015

fundamental frequency is up to 85 dB at a resolution of 300 Hz, and no any sideband is observed within a 2.5 MHz frequency range. Figure 2(d) shows the RF spectrum up to a frequency of 2 GHz at a resolution of 10 kHz, which provides further evidence of a clean, single-pulsing mode-locking state in the Erbium-doped fiber laser. Figure 2(e) shows the autocorrelation trace of the direct output pulse with a width of 233 fs, corresponding to a pulse width of 165 fs for Gaussian profile approximation.

If the bidirectional pump power is greater than 550 mW (the backward pump laser is 550 mW and the forward one is 0 mW) and the waveplates in the cavity are finely adjusted, it is possible to split the single mode-locked pulse into two or more uniformly spaced pulses. Figure 3 shows the dependence of the laser's average output power (black) and harmonic number (blue) on the bidirentional pump power. As the pump power is increased from 550 mW to 1450 mW, HML operation occures from the 2th harmonic (166.7 MHz) to the 8th harmonic (666.7 MHz). The average output power is increased from 50.2 mW to 134 mW. It is worth noting that the half waveplate needs to be adjusted precisely to get stable high-order HML with equal amplitude and spacing simultaneously. Meanwhile, once a stable harmonic mode-locking is established, its order is maintained to some extent while we decrease the pump power, resulting in hysteresis phenomena [29]. In the experiment, we also verified the effect of the forward pumping and backward pumping on laser performance. We found that in three cases ((forward, backward) = (550, 350), (475, 475), and (0, 950), respectively.) of the same total pump power, the harmonic order of the fiber laser does not change. But the laser performance has subtle difference. For example, higher backward pump power can generate more laser output power than higher forward pump power and the differences is about 2~3mW.

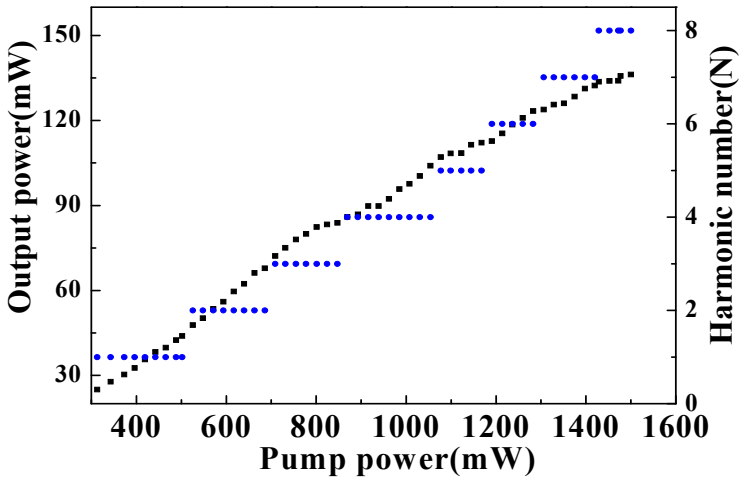

Fig. 3. The average output power (black) and the harmonic order number (blue) for different bidirectional pump power.

Figure 4(a) shows the pulse train at the highest stable repetition rate of 666.7 MHz, which corresponds to the 8th harmonic of the fundamental repetition frequency. This harmonic is obtained at the maximum available pump power of 1.5 W (the forward pump laser is 550 mW and the backward one is 950 mW). The laser output power is 136 mW, which corresponds to pulse energy of 0.2 nJ. Figure 4(b) shows the optical spectrum of the laser output at 8th HML with a FWHM of about 181 nm (from ~1460 nm to ~1630 nm). The spectrum is broad in HML due to the effective dispersion and nonlinearity optimization in the cavity and the strong pulse shaping effect significantly contributed by NPE. The pulse spectrum also includes a small cw component due to the energy coupling between the pulses and the dispersive wave in the cavity [12, 30]. Usually, the super-mode suppression ratio (SMSR) is used to evaluate

#243942 Received 30 Jun 2015; revised 31 Jul 2015; accepted 4 Aug 2015; published 6 Aug 2015

the PHML by analysis of the RF spectrum of the output pulse. Figure 4(c) shows the RF spectrum of the 8th HML pulse (666.7 MHz) when the maximum pump power of 1.5 W is applied. The SNR is suppressed to ~75 dB at a resolution of 300 Hz within a wide frequency range of larger than 100 MHz and the SMSR is larger than ~60 dB. Figure 4(d) presents the RF spectrum up to a frequency of about 10 GHz at a resolution of 10 kHz, which verifies the high stability of the HML.

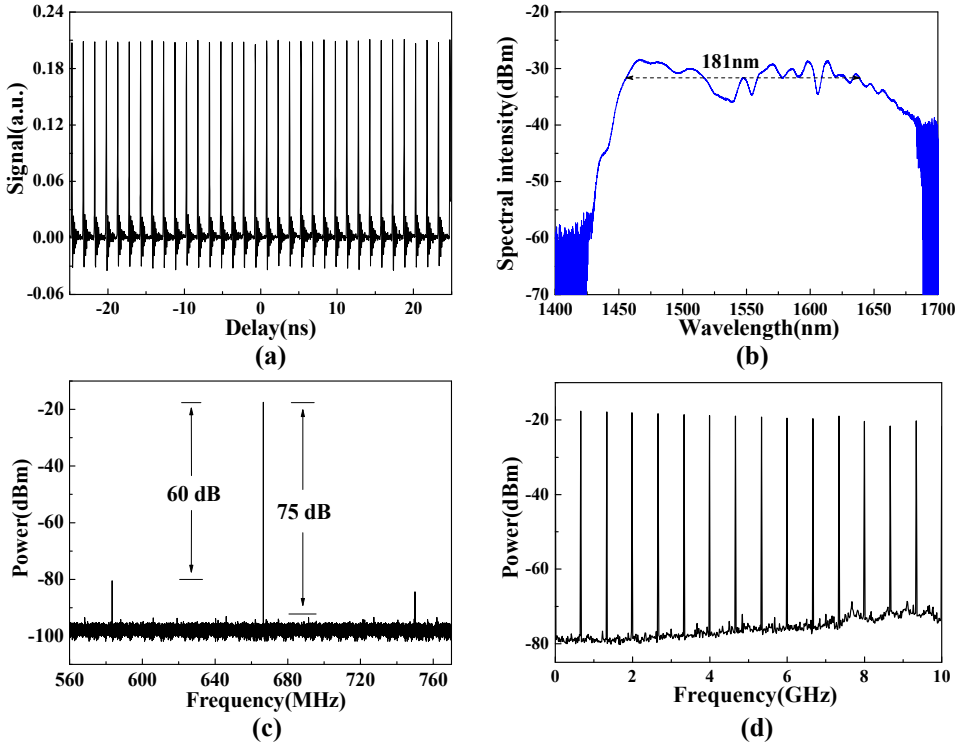

Fig. 4. The 8th hybrid HML characteristics. (a) Output pulse trains at 666.7 MHz repetition rate, (b) optical spectrum measured with 0.02 nm resolution, (c) RF spectrum measured at 300 Hz resolution bandwidth, and (d) RF spectrum with 10 GHz span at 10 kHz resolution bandwidth.

Figure 5 presents the autocorrelation trace of the 8th HML pulses (black dashed curve). No pedestal beats is observed in both sides of the pulses, indicating that temporal beat pedestals are successfully suppressed by nonlinear amplitude modulation in the oscillator with the assistance of the SESAM. The red dotted curve is a fitting by a Gaussian profile. The autocorrelation trace has a width of 308 fs corresponding to pulse width of 218 fs. Since the spectrum is very broad covering the wavelength range from 1460 nm to 1640 nm, the cavity net GVD is approximately maintained to be near-zero only at 1550 nm wavelength. Therefore, we deduce that the direct output pulse still contains some residual dispersion chirp. It is compressed to 91 fs by use of a SF10 Brewster prism pair laid outside the cavity, which is also superposed in Fig. 5 (blue solid curve). The time-bandwidth product of the compressed pulse is 2.059, which is much higher than the Fourier transform limit value of 0.441. The Fourier transform of the spectrum is plotted in comparison with the experimental dechirped pulses (gray solid curve). The transform-limited pulse width is only 43 fs, which indicates that the effect of pulse compression is not ideal. It is possibly because the presence of larger nonlinear chirp and third-order dispersion cannot be extensively compensated by the lens. The pulse width might be further compressed to below 50 fs by employing the incorporation

#243942 Received 30 Jun 2015; revised 31 Jul 2015; accepted 4 Aug 2015; published 6 Aug 2015

of grating and prism compressor [31], which is now under investigation. The peak power of the dechirped pulse is approximately 2.1 kW based on the pulsewidth (91 fs) and pulse energy (0.2 nJ). The zoomed-in view of the pulse's top is also shown in the inset of Fig. 5. From the inset we can see that the Gaussian fit top does not match the top of the direct output pulse very well and there are some components at the top of the pulse. It indicates that the output pulses are not clean enough in the harmonic mode-locking regime. It is worth further study in the future to improve the quality of the generated pulses.

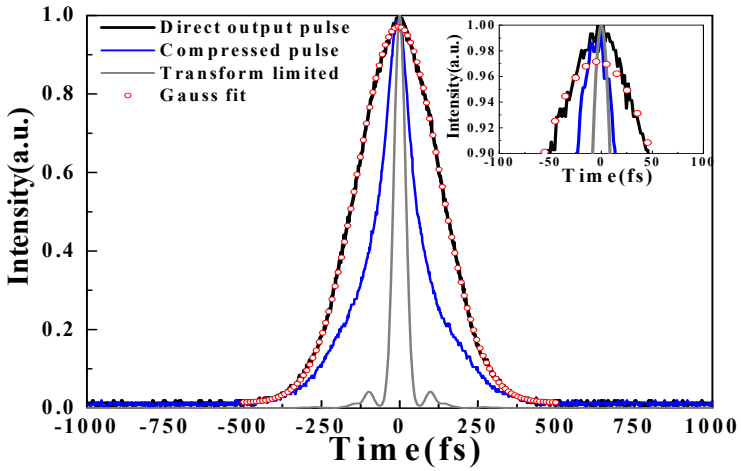

Fig. 5. The autocorrelation trace of the direct output pulse (black solid curve) and its compressed pulse (blue solid curve) at the 8th harmonic mode-locking. The gray solid curve is the Fourier transform of spectrum. A Gaussian fit curve (red dotted curve) is superimposed. The zoomed-in view of the pulse's top is shown in the inset.

In addition, at the 4th-order HML, the pulse train, optical spectrum, RF spectrum are shown in Fig. 6. The repetition rate of the output pulses is 333.3 MHz (see Fig. 6(a)). The spectrum is centered at 1542 nm with a FWHM of about 189 nm (see Fig. 6(b)). The SNR of the fundamental frequency is suppressed to ~75 dB at a resolution of 300 Hz within a frequency range of 3.5 MHz (see Fig. 6(c)). Figure 6(d) illustrates the RF spectrum up to a frequency of 3 GHz at a resolution of 10 kHz, indicating that the SMSR of the 4th harmonic is also larger than ~60 dB. Figure 7 presents the autocorrelation trace of the 4th HML direct output pulse (black dashed curve), which is measured as the order of sub-200 fs. The autocorrelation trace of the compressed pulse is also shown in Fig. 7 (blue solid curve) with the minimum pulse duration of 75 fs. The zoomed-in view of the pulse's top is also shown in the inset. To compare the compressed pulses with the expected theoretical ones, the transform-limited pulse width is also shown by gray solid curve in Fig. 7 with a pulse width of 29 fs. The time-bandwidth product of the compressed pulse is 1.777, which is smaller than that of 8th-order HML. This is because the pump power required for 4th-order HML is only 950 mW, which means that the direct output pulses from the fiber laser contain small nonlinear chirp compared with the output pulses of 8th-order HML.

#243942 Received 30 Jun 2015; revised 31 Jul 2015; accepted 4 Aug 2015; published 6 Aug 2015

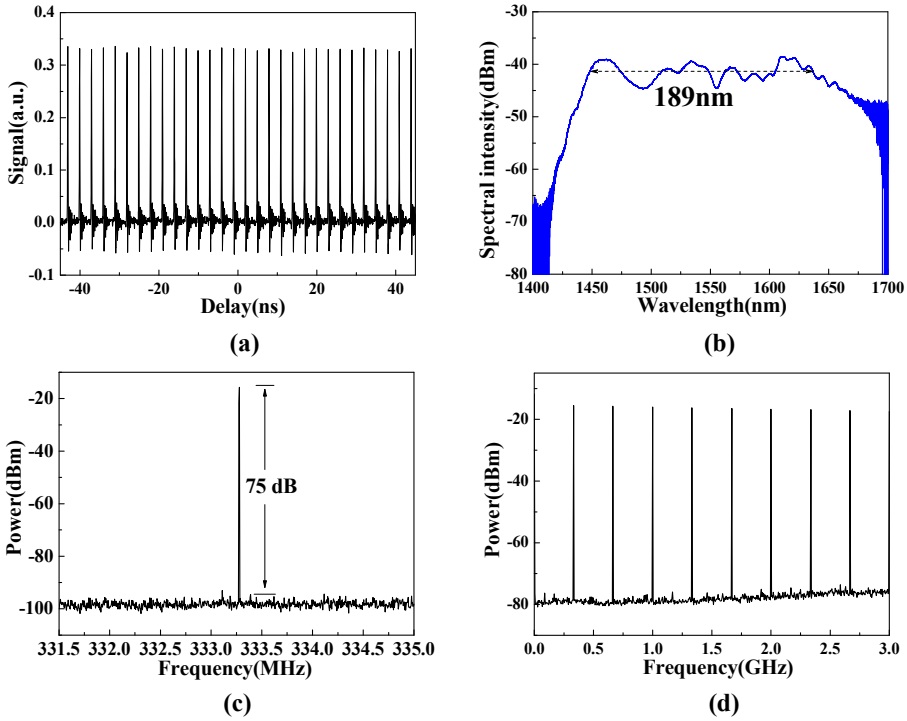

Fig. 6. The 4th hybrid HML characteristics. (a) Output pulse trains at 333.3 MHz repetition rate, (b) optical spectrum measured with 0.02 nm resolution, (c) RF spectrum measured at 300 Hz resolution bandwidth, (d) RF spectrum with 3 GHz span at 10 kHz resolution bandwidth.

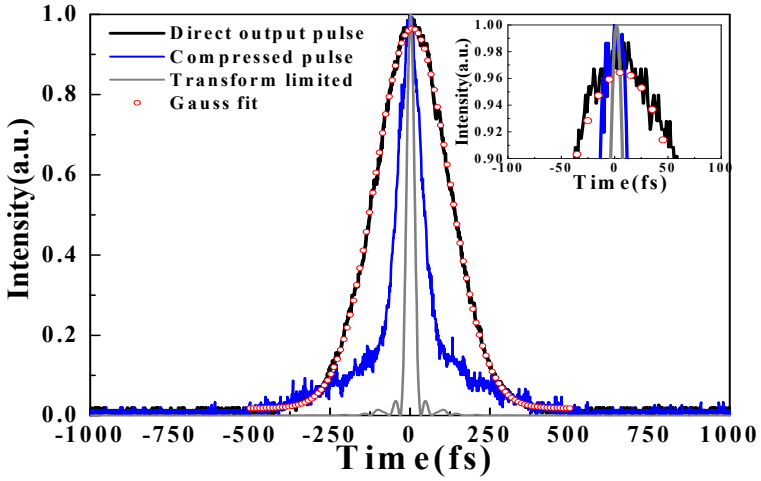

Fig. 7. The autocorrelation trace of the direct output pulse (black solid curve) and its compressed pulse (blue solid curve) at the 4th harmonic mode-locking. The gray solid curve is the Fourier transform of spectrum. A Gaussian fit curve (red dotted curve) is superimposed. The zoomed-in view of the pulse's top is shown in the inset.

4. Conclusion

In conclusion, we have demonstrated a hybrid HML fiber laser under the collaborative optimization of dispersion and nonlinearity, which is self-starting and mode-locked by a SESAM in combination with NPE. The HML fiber laser could operate with repetition

#243942 Received 30 Jun 2015; revised 31 Jul 2015; accepted 4 Aug 2015; published 6 Aug 2015

frequencies from the 2th harmonic (166.7 MHz) to the 8th harmonic (666.7 MHz) by increasing the pump power and adjusting the waveplates. For the highest repetition rate (666.7 MHz), the FWHM is 181 nm and the dechirped output pulse width is 91fs. The average output power is 136 mW and the SMSR is more than 60 dB. The compressed pulse duration of 75 fs is achieved at 333.3 MHz (the 4th HML). Under the condition of stable HML, laser operation is maintained for several hours with negligible variation of the pulse parameters. This high repetition rate and broadband fiber laser could be an excellent seed source for the photonic analog-to-digital convertor and biological imaging. However, there are still a lot of work to be undertaken in future. First, numerical simulation is very important to guide future experiments. Second, the information about pulse phase is essential to fully reflect the overall perform of the laser, so measurement by use of FROG is required. Third, the HML order of the fiber laser can be further increased by employing a compact free-space cavity configuration [32] and/or higher pump power.

Acknowledgments

This work was partially supported by National Natural Science Foundation of China (Grant Nos. 61127016 and 61007052), by SRFDP of MOE (Grant No. 20130073130005), and by the State Key Lab Project of Shanghai Jiao Tong University (Grant Nos. 2014ZZ03016).

#243942 Received 30 Jun 2015; revised 31 Jul 2015; accepted 4 Aug 2015; published 6 Aug 2015